Numerical and experimental studies of the riveting process and the strength of the riveted joints

J.-L. Chenot[1)], Nanjiang Chen[1, 2)], Min Wan[2)], Julien Malrieu[3)], Maxime Thonnerieux[3)], R. Ducloux[4)]

1) CEMEF – Mines ParisTech, BP 207 – 06 904 Sophia Antipolis Cedex / France, jean-loup.chenot@mines-paristech.fr; 2) School of Mechanical Engineering and Automation, Beihang University, 100091 / P. R China; 3) Cetim Saint Etienne, 7 rue de la presse, 42952, Satint Etienne / France; 4) Transvalor, Les Espaces Delta, BP 037 Sophia Antipolis Cedex / France

The riveting process is a very important mechanical fastening process for a wide range of applications for aerospace, car industry, etc. Today the use of rivets is mainly based on experience and some industrial laboratory tests. More recently a need for a more accurate and faster approach has emerged in order to evaluate the process of riveting and the strength of the assembly. The purpose of this paper is to illustrate some preliminary results which were obtained during the MonaLisa project. A computer code must take into account the rivet, two or more metal sheets, the riveting tools and their interactions. A three-dimensional finite element approach is considered in order to be able to treat non axisymmetric deformation, e. g. shearing of the assembly or riveting with different axes for the rivet and the sheets. The space discretization for our velocity-pressure formulation is performed using $P1^{+}P1$ tetrahedral elements. The riveting process was simulated for different rivet sizes and compared with experimental data. Different levels of material description were introduced including a map of initial hardness in the rivet and a simple damage law. The strength of the assembly was tested using a tension test.

Keywords: riveted joints, solid rivet, strength, finite element

Introduction

Riveting technique is an industrial method to achieve an assembly of two or more sheets. In a number of kinds of rivets, solid rivet is the oldest and most reliable one. It can be found in the Bronze Age [1], as well as in the modern aircrafts. Firstly complex analytical mathematical methods were used [2, 3]. More recently, thanks to the efficiency of numerical technique, abundance of works emerged almost on every aspect of the riveted joint. Blanchot et al utilized 15° sector, axisymmetric and symmetric models to simulate the riveting process and showed strain and stress distribution [4]. Bouchard et al simulated the self-pierce riveting process with Forge2005, with damage analysis, up to fracture [5]. Langrand et al dealt with the experimental and numerical characterization of dynamic failure models [6]. Liam Ryan et al studied the failure mechanism of the riveted joint [7]. However, a more systematic and comprehensive study is necessary to give confidence in the results of numerical simulation for a routine use in industry.

In this paper we have compared simulations and experiments for the riveting process, for the tensile and the shearing test of the riveted joint and the influence of several technical parameters on the riveting process. The work was carried out with two new computer codes: Riv3D for the riveting process, Join3D for the mechanical tests and Forge3.

Rivet configuration

We consider three button head rivets and one pan head rivet, the sizes of which are shown in **Table 1**.

Table 1. Initial sizes of the riveted joints (unit: mm)

Case	d	L	d_h	L_1	L_2	h (mm)
a	14.9	36	16	7.8	5.8	
b	11.6	32.4	12.5	7.8	5.8	
c	9.8	30.4	10.5	7.8	5.8	
d	5.8	15.4	6.45	2.8	2.8	3

Configurations of the tools are illustrated in **Figure 1.**

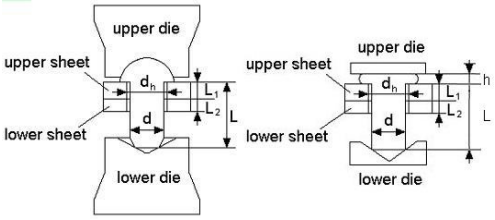

Figure 1. Configuration of the riveted joint, left one is case (a), (b) and (c) right is case (d) as shown in **Table 1**

Finite element model

In order to be able to treat the case with different axes for the rivet and the sheets, our model is 3D and generally, thanks to the symmetry of the riveting process, only one half of the rivet has to be modelled. In this study the riveting process is a cold forming process, therefore the heat effect can be neglected. Coulomb's friction law is used in the simulation and the friction coefficient between the objects is 0.15.

Constitutive parameters. To obtain the material parameters of the sheets, uniaxial tension tests of the material is performed. The rivet material is mainly subjected to compression stress during the manufacturing process, while in the tension of the riveted joint, it is mainly subjected to tensile stress. To make sure that the initial strain hardening in the shank of the rivet is uniform, a Vickers test on the initial rivets is made to obtain the hardness distribution on the section as shown in **Figure 2**.

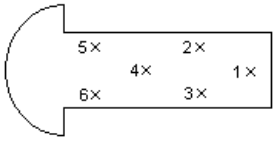

Figure 2. Hardness indentation points distribution on the section

In **Table 2** hardness values of the shank of each rivet, show that the initial strain hardening is almost uniform.

Table 2. Vickers hardness values on the section surface of the rivet for case a, b and c (unit: kg/mm^2)

Case	Point 1	Point 2	Point 3	Point 4	Point 5	Point 6
a	140	155	147	152	155	151
b	120	121	122	119	120	119
c	122	123	122	123	120	120

The true stress strain curves from the upset and uniaxial tension test are shown in **Figure 3**. The curve from the uniaxial tension test is only effective before the necking point because the strain is no longer uniform after necking happens in the experiment. Due to the Bauschinger Effect in the manufacturing process of the rivet, the curve from the uniaxial tension is lower than that from the upset test and the difference between the two curves is almost constant.

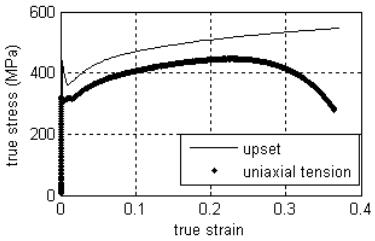

Figure 3. True stress strain from upset test and uniaxial tension test

For the rivet material, the following hardening law was found to be the most accurate one:

$$\sigma = \sqrt{3}k(1 + a\varepsilon^n) \quad (1)$$

where, σ is the yielding stress, ε is the plastic strain and k, a and n are material parameters.

Riveting process and the results

In **Table 3**, the parameters of each material are listed.

Table 3. Material parameters of the rivets and sheets used in the riveting process

Name	k (MPa)	a	n	E (GPa)	V
S235JR	242.5	0.9542	0.4796	210	0.3
FR8	194.7	1.013	0.4879	210	0.3
FR5	242.2	0.5025	0.6298	210	0.3
S700MC	242.7	0.5740	0.1300	210	0.3
HLES600MC	346.2	1.072	0.5635	210	0.3
HLES355MC	225.0	1.249	0.6660	210	0.3

All the deformed parts including the rivet and the sheets are meshed with tetrahedral elements while the surfaces of the dies are considered as rigid and meshed with triangular elements. In the riveting process, to avoid distortion of the meshes, our automatic remeshing module is utilized to remesh the critical area timely.

The displacements of the low die are controlled in the experiments and in the simulations, they are set to the following values (in mm): a: 11.5, b: 11.8, c: 11, d: 7.5.

Final configuration of the riveted joints. Figure 4 shows the final shapes of the riveted joints from the experiments and the simulations. Because the thicknesses of the sheets in each case exhibit almost no change, it can be used to calibrate the two photos from experiment and from simulation. In **Figure 4**, the final shapes of the riveted joints from the simulations are almost the same as those from the experiments.

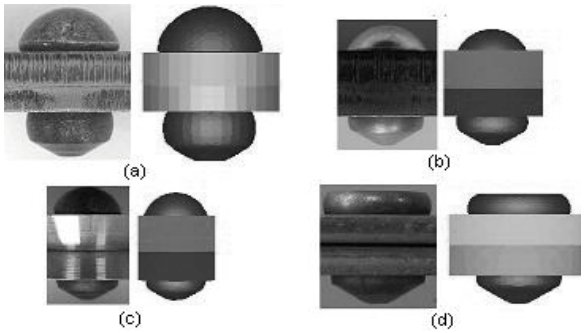

Figure 4. Comparison of final shapes of the riveted joints between experiments (left) and simulations (right) for the four cases

To compare the inner shape of the joint, one of the 15mm riveted joint is cut into two pieces. In **Figure 5**, we see that the results from the simulation and from the experiment have the same final shape.

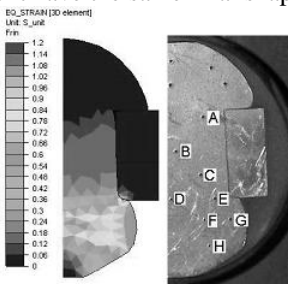

Figure 5. the cross section of the riveted joint of case (a), the left part is from the simulation while the right part is from the experiment

The height and the diameter of the head, as shown in **Figure 6,** are the two important parameters which are compared in **Table 4** for both the simulation and the experiment (average value of several samples). For all the four cases, the biggest error is less than 4%.

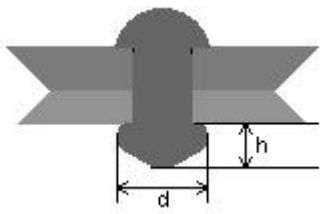

Figure 6. The two important parameters of the forming head

Table 4. Comparison of the finals shape of the forming head

Case	h (mm)			d (mm)		
	exp	sim	Error	Exp	sim	Error
a	12.35	12.34	-0.1%	21.51	21.00	-2.3%
b	8.84	9.11	3.1%	18.79	18.36	-2.3%
c	7.8	7.63	-2.2%	16.05	16.32	-1.7%
d	10.5	10.6	1.0%	3.3	3.4	3.0%

Relationship between load and displacement of the lower die. The relationship between the riveting load and the displacement of the lower die is one of the engineers' major concerns. It shows how much load is needed to obtain a given kind of forming head, which is determined by the displacement of the lower die. In **Figure 7** the load displacement curves during the riveting process are drawn for the four riveted joints. The comparison between the curve from Riv3D, or Forge3, and that from the experiment for each case is excellent. In each figure, there are two apparent turning points in each curve: the first one at A, is due to yielding of the rivet material, while the second one at B is because the expansion of the rivet shank starts to contact the wall of the hole of the sheets.

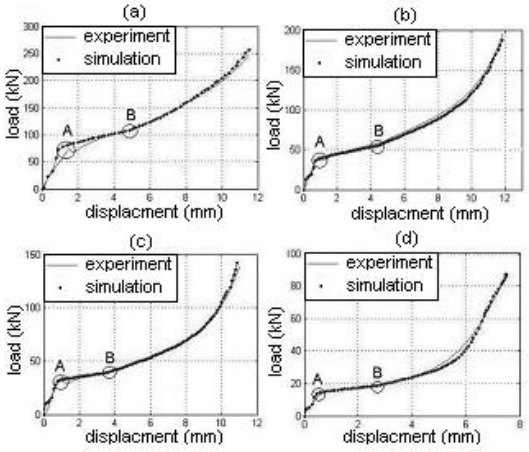

Figure 7. Load displacement curve from experiment and from simulation

Comparison of the hardness distribution between experiment and simulation for case a. According to Tabor [9], the Vickers' hardness is proportional to the yield stress:

$$Hv = c\sigma(\varepsilon_0 + 0.08) \quad (2)$$

where, Hv is the Vickers' hardness in MPa, c is a constant usually equals to 3, ε_0 is the local equivalent strain of the metal and $\sigma(\varepsilon_0+0.08)$ is the yielding stress in MPa at equivalent strain $(\varepsilon_0+0.08)$.

In order to obtain the work hardening information of the inner material of the rivet after the riveting process, the rivet of case a in **Table 1** was selected to be cut into two pieces along the longitudinal direction. As shown in **Figure 5**, since the driven head had more complicated deformation than the shank of the rivet, more test points are located in this part to better illustrate the hardness distribution of the rivet. In the experiment, 9 points of the right part of the rivet were selected to obtain the Vickers hardness. Correspondingly, in the simulation result, the equivalent strain of the points having the same coordinates as the points in the experiments were obtained and then the hardness of all points was calculated using Equation (2) and Equation (1). The comparison results are shown in **Table 5**. The absolute errors of all points between the simulation and the experiment are all less than 10%.

Table 5. Comparison of the hardness distribution in the riveted joint between the simulation and the experiment for case a

Point	Hardness in experiment (kg/mm^2)	Simulation		Error (%)
		Strain	Hardness (kg/mm^2)	
A	169	0.07	181.64	7.48
B	184	0.16	189.17	2.82
C	182	0.17	189.88	4.33
D	189	0.31	198.05	4.79
E	202	0.38	201.35	-0.32
F	242	0.92	219.06	-9.48
G	223	0.77	215.03	-3.57
H	212	0.62	210.45	-0.73

Tension process of the riveted joint for case c and the result

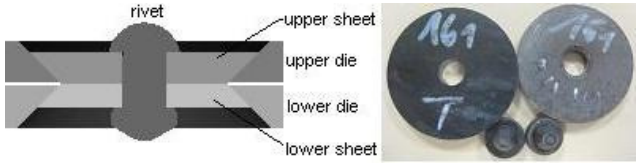

(a) Assembly for tension (b) after tension

Figure 8. The illustration of the tension of the riveted joint (a) and the sample (b) after tension test in the experiment

To obtain the tensile strength of the riveted joint, the lower die is fixed while the upper die moves in the axis direction of the rivet. The sample of case c after tension in **Figure 8** shows that the shank of the rivet is subjected to the tensile stress and the deformation locates mainly in this part. Hence, in the simulation, the material parameters from the uniaxial tension should be utilized in this process. Furthermore, the shank breaks during the tension process of the riveted joint, so the damage model is necessary to be taken into account in the simulation. In view of the importance of the largest tensile stress, Cockcroft and Latham [10] proposed a fracture criterion based on critical value of the tensile strain energy per unit volume. The normalized version can be written as:

$$\int_0^{\bar{\varepsilon}_f} (\sigma_1 / \overline{\sigma}) d\bar{\varepsilon} = C \quad (3)$$

where, σ_1 is the largest tensile stress, $\overline{\sigma}$ is the equivalent stress and C is a material parameter set equal to 1.5 after iterative simulations.

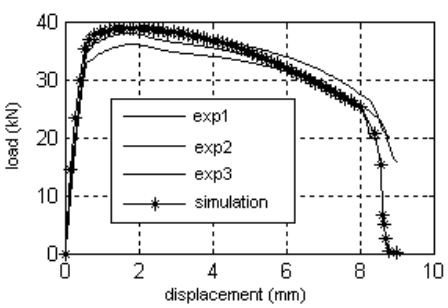

Figure 9. The load displacement curves of tension from the simulation and from the experiments for case c.

Relationship between the load and the displacement

of the upper die for the tension of the riveted joint. The comparison of the load and displacement between experiments and simulations is quite good even if, in **Figure 9,** the maximum load in the simulation is slightly overestimated. One reason for this phenomenon may be that, in the simulation, the material parameters are determined from the uniaxial tension of the rivet while, due to Bauschinger effect, the compressive riveting process may decrease the tensile strength.

Shearing process of the riveted joint for case d and the result

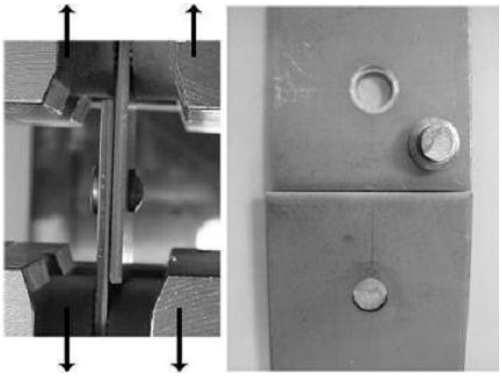

(a) Assembly for shearing (b) after shearing

Figure 10. Shearing of the riveted joint (a) and the sample (b) after shearing test in the experiment

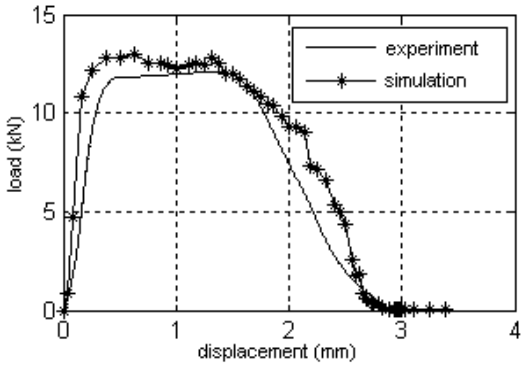

Figure 11. Load displacement curves of the shearing from the simulation and from the experiments for case c.

To test the shearing strength of the riveted joint, the end of each sheet is clamped by the press machine and then the press machine moves in the direction as shown in **Figure 10.** For the shearing test, the material parameters are also the ones from the uniaxial tension test and the damage model is Cockcroft and Latham law the same as that used in the tension test. The constant value C in equation (3) is 0.5, using the same method as that in the tension test.

Relationship between the load and the displacement of the upper die for the shearing of the riveted joint. Figure 11 shows the load and displacement from the experiment and from the simulation with a good agreement.

Parameters influence on the riveting process for case d

In the reality, especially in the industry, the initial conditions including the geometry of the rivets, the assembly positions, etc, are not possible to be set as same as those in the experiment. Hence, by varying those parameters, it is important to study their influence on the simulations. In this study, the parameters of case d in **Table 1** are set as the standard ones and in each batch only one parameter is changed. In **Table 6** are the results where d is the diameter of the rivet, L is the length of the rivet, d_h is the diameter of the hole of the sheets, L_1 and L_2 are the thickness of the upper sheet and the lower sheet respectively. When the friction coefficient between the lower die and the rivet changes from 0 to 0.45, the load displacement curve has almost no variation compared with result with the value 0.15.

Table 6. Geometrical parameters' influence on the maximum force in the riveting process for case d

Parameters	Change (%)	Change of max force (%)
d	-3	-12.4
L	-3	12.1
d_h	-3	4.1
L_1=L_2	-3	-5.2

Conclusions

The F. E. simulations of the riveting process and of the mechanical test of the assembly were carried out. It shows that the results reproduce accurately the experimental measurements, including the configurations of the riveted joints, the load displacement curves and the hardness distribution on the longitudinal section of the rivet after riveting. A sensitivity analysis allowed us to asses the variations of the riveting parameters to the initial geometry.

Acknowledgement

This work is a part of the MonaLisa project, financed by Cetim with a close cooperation between Cetim, Cemef and Transvalor.

References

[1]http://sketchup.google.com/3dwarehouse/details?mid=23736e9c33cc79d0eab2bd7322386ffd&ct=lc&hl=fr
[2] H. Huth, Fatigue in Mechanically Fastened Composite and Metallic Joints, ed. By J.M. Potter, ASTM SPT 927 (1986), p. 221-250
[3] Y. Xiong, Int. J. of Solid & Structure, vol. 33, 29 (1996), p. 4395-09
[4] V. Blanchot & A. Daidie, Journal of Materials processing Technology. 180 (2006), p. 201-9
[5] P.O. Bouchard, T. Laurent & L. Tollier, Journal of Materials processing Technology. 202 (2008), p. 290-300
[6] B. Langrand, E. Deletombe, E. Markievicz and P. Drazetic, Numerical approach for assessment of dynamic strength for riveted joints, Aerospace Science Technology 3 (1999), p. 431-46
[7] Liam Ryan and John Monaghan, Journal of Materials processing Technology. 103 (2000), p. 36-43
[8] S. Akhtar, K. Khan & M. Jackson, International journal of plasticity. 15 (1999) p. 1265-75
[9] D. Tabor, The Hardness of Metals, Oxford, Clarendon Press, (1951) p. 105-107
[10] J. Landre et al. Finite Elements in Analysis and Design, 39 (2003), 175-86